Journal of Power Sources 196 (2011) 988–998

Contents lists available at ScienceDirect

Journal of Power Sources

journal homepage: www.elsevier.com/locate/jpowsour

Preparation and characterization of phosphotungstic acid-derived salt/Nafion nanocomposite membranes for proton exchange membrane fuel cells

M. Amirinejad[a], S.S. Madaeni[a,*], M.A. Navarra[b], E. Rafiee[c], B. Scrosati[b]

[a] Membrane Research Center, Department of Chemical Engineering, Faculty of Engineering, Razi University, Tagh Bostan, Kermanshah, Iran
[b] Department of Chemistry, University of Rome "La Sapienza", 00185 Rome, Italy
[c] Department of Inorganic Chemistry, Faculty of Chemistry, Razi University, Kermanshah, Iran

ARTICLE INFO

Article history:
Received 19 August 2010
Accepted 20 August 2010
Available online 19 September 2010

Keywords:
Nanocomposite membrane
Nafion
Proton exchange membrane fuel cell
Heteropolyacid
Conductivity

ABSTRACT

Nafion/$Cs_{2.5}H_{0.5}PW_{12}O_{40}$ nanocomposite membranes are prepared and characterized as alternate materials for PEMFC operation at high temperature/low humidity. The $Cs_{2.5}H_{0.5}PW_{12}O_{40}$ solid acid particles (hereafter CsPWA) have the high surface area, the high hygroscopic property and the ability to generate proton in the presence of water molecules. The results of prepared membranes at three levels (0, 10 and 15%) indicate that the CsPWA particles have influence on the water content, ion exchange capacity, thermal properties (TGA and DSC), proton conductivity and PEM fuel cell performance. Particles agglomeration and Nafion active sites (sulfonic groups) covering are seen in the nanocomposite membranes. The conductivity of nanocomposite membranes at high temperatures (110 and 120 °C) is higher than plain Nafion and may be related to the additional water within the nanocomposite membrane and/or the additional surface functional site provide by CsPWA. The fuel cell responses show that in the fully hydrated state and at the higher current densities, the prepared MEAs with nanocomposite membranes possess better response compared with the plain Nafion. In partially hydrated cell, at both low and high current densities, the superior performance of the MEA prepared by nanocomposite membranes is observed.

1. Introduction

Nafion as the major type of commercially available membrane for DMFC and PEMFC is durable and has high ionic conductivity at normal temperatures. The hydrophobic polytetrafluoroethylene (PTFE) backbone of Nafion provides thermal and chemical stability whereas the hydrophilic sulfonic acid ($-SO_3H$) provides channels for proton conduction [1,2]. At high temperature and low humidity operations, Nafion membrane dehydrates and its conductivity decreases dramatically. The design of proton conducting membranes being stable and providing good performance above 100 °C presents a major challenge [3]. Operation at temperatures above 100 °C is useful for PEM fuel cells to enhance reaction kinetics, improve thermal management, heat utilization, simplify water management and increase CO tolerance [4–6]. Approaches adapted to increase PEMFC operating temperatures are detailed in recent reviews [3,7,8].

Improvements to the structure and functionality of Nafion membrane are usually made by adding inorganic or organic constituents. The class of these membranes is referred as perfluorinated ionomer composite membrane (PFICM) [7]. Based on the structure of additives, macrocomposite and nanocomposite membranes have been developed. Macrocomposite and nanocomposite membranes are the combination of the polymer with organic or inorganic structures of micro-meter or nano-meter scales, respectively. The recent additives reported to promote Nafion properties are listed in Table 1. These additives may be utilized as acid sites (PWA, SiWA, PMoA and SiMoA), water retention amplifier (ZrP), structure modifier (zeolite), electronic conductors (polyaniline and polypyrrole) or catalysts for proton transport (Pt–Sn and Pt–PDDA–PTFE). In DMFC, the main advantage of additives is to decrease methanol crossover.

The water sorption and proton transport of PFICMs depend on the size, uniform dispersion, loading content and acid sites amount of particles. Moreover, PFICMs properties may be influenced by the compatibility and interactions of Nafion with particles [88,89].

The main features of interest of heteropolyacids (HPAs) are their structure and their strong acidity [90]. HPAs in the solid state are pure Brønsted acids stronger than the conventional solid acids such as SiO_2, Al_2O_3, and zeolites. The most common local structure is the Keggin form. This structure is formed by a central atom (Si or P) tetrahedrally linked to oxygen and surrounded by oxygen-linked peripheral metal atoms (Mo, W, V, Co, etc.) or a combination of them. The primary $PW_{12}O_{40}^{3-}$ Keggin anion (Fig. 1a) composed

* Corresponding author. Tel.: +98 831 4274530; fax: +98 831 4274542.
E-mail addresses: amirinejad@razi.ac.ir (M. Amirinejad), smadaeni@yahoo.com (S.S. Madaeni), mariassunta.navarra@uniroma1.it (M.A. Navarra), e.rafiei@razi.ac.ir (E. Rafiee), bruno.scrosati@uniroma1.it (B. Scrosati).

0378-7753/$ – see front matter © 2010 Elsevier B.V. All rights reserved.
doi:10.1016/j.jpowsour.2010.08.062

Table 1
Recent literature reviews on Nafion-composite membranes for PEMFCs and DMFCs.

PEMFC	Reference	DMFC	Reference
Polytetrafluoroethylene (PTFE)	[9–13]	SiO_2	[52–54]
Zeolite	[14]	Organic-SiO_2	[55,56]
Phosphotungstic acid (PWA), silicotungstic acid (SiWA), phosphomolybdic acid (PMoA), silicomolybdic acid (SiMoA)	[6,15,16]	ZrP	[57,58]
Cs-modified-PWA	[17]	Calcium phosphate (CaP)	[59]
Inorganic oxides (SiO_2, TiO_2, ZrO_2, WO_3)	[18–25]	SiO_2/ZrP/TiP (titanium phosphate)	[60]
Titanate-nanotube	[26]	SiO_2/TiO_2	[61]
TiO_2/montmorillonite	[27]	Sulfonated-organosilica	[62]
Bifunctional silica	[28]	Diphenylsilicate	[63]
Silica/sulfuric acid	[29]	Sulfonated-titanate	[64]
Sulfated-zirconia	[30,31]	Sulfonated polyethylene-alt-tetrafluoroethylene (ETFE-SA)	[65]
Sulfonated-montmorillonite	[32]	PTFE	[66]
Clay-SO_3H	[33]	PTFE/SiO_2	[67]
Zirconium phosphate (ZrP)	[34,35]	PTFE/ZrP	[68]
Zirconium sulfophenyl phosphate (ZrSPP)	[36]	H-ZSM-5 zeolite	[69]
Phospho silicate (SiP)	[37]	Clay	[70]
Calcium-hydroxyphosphate	[38]	Montmorillonite	[71]
Fullerene ($C_{60}(OH)_n$, $n \sim 12$)	[39]	Bio-functionalized montmorillonite	[72]
SiO_2/PWA	[40,41]	Erbium triflate (ErTfO)	[73]
Metal dioxide supported-PWA	[42]	Polypyrrole	[74–76]
HPW-SiO_2	[43]	Polyvinylidene fluoride (PVdF)	[77]
SiO_2/triethylammonium trifluoromethanesulfonate (TEATF)	[44]	Polyaniline	[78]
SiO_2/Pt	[45]	Polybenzimidazole	[79]
CdS + PbS	[46]	Polyfurfuryl alcohol	[80]
Pt–Sn	[47]	Polyimide (PI)	[81]
Pt–polydiallyldimethylammonium chloride(PDDA)–PTFE	[48]	3-Mercaptopropyl methyldimethoxysilane (MPMDMS)	[82]
$SiO_2/P_2O_5/ZrO_2$	[49]	Sulfonated polyarylene ether ketone (SPAEK)	[83]
Polyaniline	[50]	Poly(p-phenylene vinylene)	[84]
Polypyrrole	[51]	SiO_2/polyaniline	[85]
		Polyvinyl alcohol (PVA)/chitosan	[86]
		PI/PVA/TSPS (8-trimethoxysilylpropyl glycerin ether-1,3,6-pyrenetrisulfonic acid)	[87]

of a central tetrahedron PO_4 surrounded by 12 edge- and corner-sharing metal-oxygen octahedra WO_6. The octahedra are arranged in four W_3O_{13} groups. Each group is formed by three octahedra sharing edges and having a common oxygen atom which is also shared with the central tetrahedron PO_4 [91]. The secondary structure is a three-dimensional arrangement consisting of primary structure, cations, water of crystallization and other molecules [92]. The tertiary structure is assembled solid HPAs. The tertiary structure is very influential on the properties of solid HPAs such as particles size, pore structure and distribution of protons in the particle [93].

Perfluorosulfonic acid-based organic/inorganic composite membranes with different heteropolyacid (HPA) additives have been investigated as alternate materials for low humidity PEMFC operation [6,15–17,40–43]. The major factor limiting the performance of Nafion/HPA composite membranes is the high solubility of the HPA additive. Water-insoluble salts with large monovalent cations such as Cs^+ have strong acid sites, rigid microporous/mesoporous structure and high surface area [94]. Lee et al. has shown by the temperature programmed desorption (TPD) of ammonia that $Cs_{2.5}H_{0.5}PW_{12}O_{40}$ (hereafter CsPWA) and PWA have similar acid strength [95]. The surface area, pore size and pore volume of CsPWA are 128 $m^2\,g^{-1}$, 30 Å and 0.095 $cm^2\,g^{-1}$, respectively as reported elsewhere [96]. The primary, secondary and tertiary structures of CsPWA are shown in Fig. 1. The $PW_{12}O_{40}{}^{3-}$ polyanions are bridged by Cs^+ cation. It is shown that proton of CsPWA is distributed uniformly through the solid bulk. This distribution is based on the study of relative intensities of P NMR peaks performed by Mizuno and Misono [92].

In this study, CsPWA was utilized as a proton conducting additive to modify the Nafion membrane and produce stable nanocomposite at moderate temperature and low relative humidity.

2. Experimental

2.1. Materials

LIQUION solution (LQ-1105) with EW = 1100 and d = 0.86 g cm^{-3} was purchased from Ion Power, Inc. is a dispersion (5 wt.%) of Nafion in a mixture of water and alcohols. N,N-Dimethylacetamide (hereafter DMAc) was obtained from Fluka. Sodium chloride 98% and sodium hydroxide were supplied from Aldrich. Hydrogen peroxide (40% m/v in water) and sulfuric acid 96% with density = 1.835 g mL^{-1} were acquired from Carlo-Erba. Phosphotungstic acid hydride and cesium carbonate were obtained from Merck.

2.2. Preparation of CsPWA

CsPWA was prepared by precipitation titration as described elsewhere [97]. The aqueous solutions of $H_3PW_{12}O_{40}$ (0.08 M) and Cs_2CO_3 (0.1 M) were prepared. Cs_2CO_3 solution was added to 20 mL of $H_3PW_{12}O_{40}$ solution dropwise with stirring in room temperature. The milky colloidal solution was stirred overnight and then liquid phase was evaporated at 45 °C. CsPWA powder was obtained by heating at 300 °C for 1 h. This powder was grinded and dried in vacuum oven at 80 °C and stored in an inert and dry atmosphere before use. The proposed mechanism of preparation process of CsPWA can be found in [98].

2.3. Preparation of membranes

Nanocomposite membranes were prepared by recast procedure. The solvents of Nafion solution were exchanged gradually by DMAc at 80 °C. DMAc has a higher boiling point and solubility parameter than water and isopropyl alcohol. CsPWA powder was added to

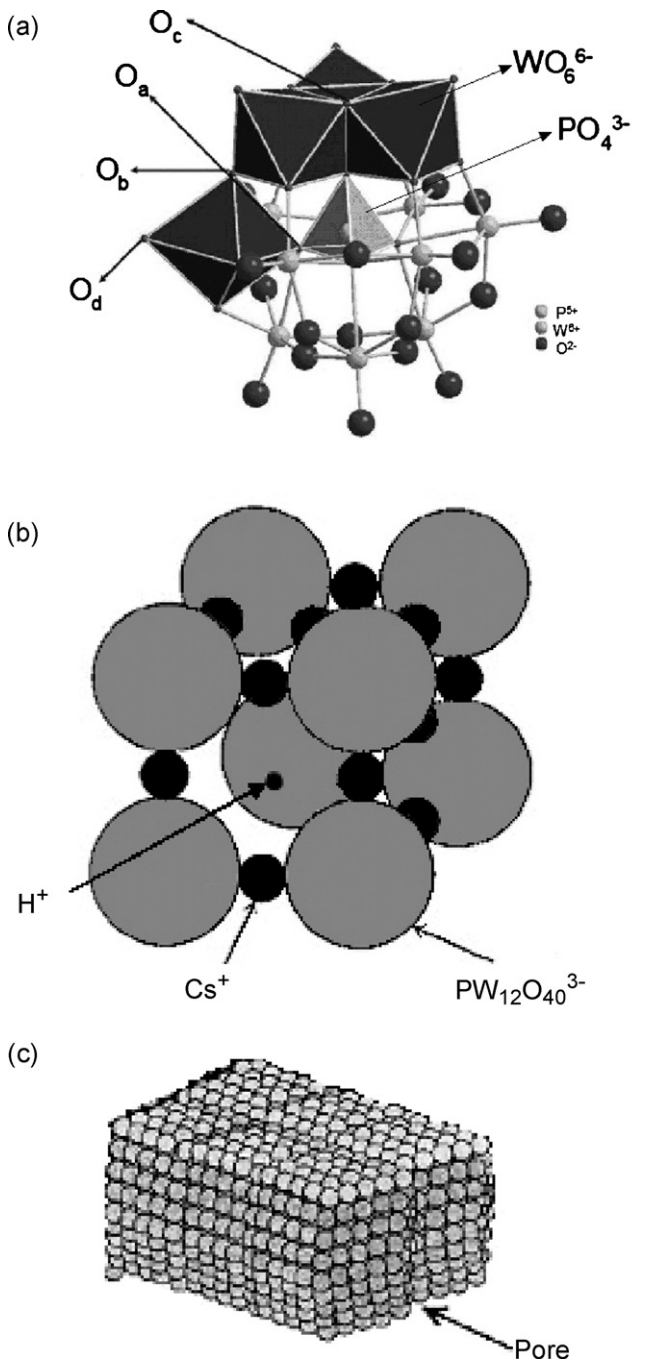

Fig. 1. Primary (a), secondary (b) and tertiary (c) structures of CsPWA.

the solution discreetly with stirring to avoid salt agglomeration. The concentration of filler was calculated with respect to Nafion polymer weight. The solution was mixed for at least 24 h. The homogenously dispersed and viscose solution was poured onto a Petri dish and the solvent evaporated at 100 °C. Dried membranes were peeled off from the surface and subjected to the next stage. For comparison purposes, recast Nafion membranes without inorganic filler were also prepared by the same procedure.

2.4. Membranes cleaning

In order to remove the organic and inorganic impurities and to reach complete protonation, the prepared membranes were boiled in H_2O_2 3 w/v% for 90 min and then in H_2SO_4 0.5 M for 90 min. The membranes were finally washed in boiling deionized water for 90 min. The membrane samples were stored in fresh deionized water before measurements.

2.5. Fourier transform-infra red (FT-IR) analysis

The infrared spectra on CsPWA salt powders in the region of 400–4000 cm^{-1} were recorded in KBr pellets using a BRUCKER vector 22 FT-IR spectrophotometer. The spectrum obtained after multiple scans was a plot of transmittance percent against wavenumber.

2.6. Morphological study

Morphological study of the salt was investigated by scanning electron microscopy, SEM LEO 1450VP apparatus.

2.7. Thermal gravimetric (TG) and derivative thermal gravimetric (DTG) analyses

Thermal gravimetric analysis was investigated by TGA/SDTA 851 Mettler-Toledo instrument. TGA was performed from 25 to 600 °C by air flux of 60 mL min^{-1} with the scan rate of 20 °C min^{-1} for 25–300 °C and the scan rate of 10 °C min^{-1} for 300–600 °C.

2.8. Differential scanning calorimetry (DSC) analysis

Differential scanning calorimetry of the membranes were studied by DSC 821 Mettler Toledo with nitrogen flow rate of 70 mL min^{-1} and scan rates of 5 °C min^{-1} for the cycle of 25 °C (−125 °C) to 25 °C and 20 °C min^{-1} for the cycle of 25 °C (280 °C) to 25 °C. DSC was performed quickly when the surface water was removed.

2.9. Water uptake

Water uptake (wu) property of membranes in the room temperature was determined by the following formula:

$$\text{wu}\ (\%) = \frac{W_{\text{wet}} - W_{\text{dry}}}{W_{\text{dry}}} \times 100 \quad (1)$$

where, W_{wet} is the membranes weight after cleaning and when the surface water was removed and W_{dry} is the membranes weight after drying at 70 °C.

2.10. Ion exchange capacity (IEC)

IEC was performed by classical titration. Dried membranes were immersed in NaCl 0.1 M aqueous solution and the H^+ was titrated by NaOH 0.004 N aqueous solution. The IEC was measured at least two times and the average is reported.

2.11. Proton conductivity

Proton conductivity was evaluated by AC impedance technique, accomplished with Frequency Response Analyzer, FRA 1255B Solartron. A signal of 10 mV amplitude in the frequency range of 100 kHz to 1 Hz was applied to the screwed cell where the given membrane sample was sandwiched between two electrodes. The electrodes were commercial E-Tek carbon cloths with 0.5 mg Pt cm^{-2} loading. The humidity and temperature of the cell were controlled inside a cylindrical chamber. This cylindrical chamber included two lower and upper compartments contained liquid water and vapor, respectively. The compartments equipped separately with heaters, thermocouples and temperature controllers and indicators. The lower and upper compartments

Table 2
General properties of the prepared membranes.

Entry	Membrane	$Cs_{2.5}H_{0.5}PW_{12}O_{40}$ content (%)	Mean thickness (μm)	Color	Room temperature conductivity ($S\,cm^{-1}$)
1	Recast-Nafion	0	80	Transparent	1.7×10^{-3}
2	10-CsPWA/Nafion	10	70	Opaque	2.3×10^{-3}
3	15-CsPWA/Nafion	15	90	Opaque	3.4×10^{-3}

provided desired vapor pressure and vapor temperature, respectively. Desired humidity and temperature were achieved by the temperature differences in the upper and lower compartments. The humidity values were indicated by a humidity sensor provided on the top of upper compartment. The conductivity cell was placed in the upper compartment. This cell was porous and metallic to reach more quickly to the humidity and temperature inside chamber. The cells were allowed to reach steady state for a few hours before taking any measurement. The proton conductivity (σ, $S\,cm^{-1}$) of membranes was calculated using the following equation:

$$\sigma = \frac{L}{RS}$$

where L, R and S are the thickness (cm), the impedance (Ω) and the surface area (cm^2) of the membranes, respectively. R was obtained from intercept of the linear or the semicircle with the Re (z) axis.

2.12. MEA fabrication and PEM fuel cell performance

PEM fuel cell tests were performed by using a compact system, 850C Scribner Associates Inc. with a cell hardware, having an active surface of $5\,cm^2$, connected to this system. Commercial electrodes, E-Tek, Teflon treated carbon cloths as gas diffusion layer with 0.5 mg Pt cm^{-2} loading were used. These electrodes were brushed with Nafion solution (LIQUION) ~0.9 mg cm^{-2} loading. Membrane electrode assembly (MEA) was fabricated by hot-pressing electrode–membrane–electrode at 120 °C and 2 atm for ~7 min. Hydrogen (fuel) and air (oxidant) with the pressure of 1 atm, desired humidity and the flow rates a bit higher than stoichiometric flows were fed to the system. Desired humidity was achieved by changing the temperatures of the humidifier and the cell.

3. Results and discussion

The abbreviation, mean thickness, color and conductivity (room temperature/humidity) related to the prepared membranes are represented in Table 2. The nanocomposite membranes were milky color and opaque. The room conductivity values are in order of 10^{-3}. The conductivity of composite membranes at room temperature is slightly higher than plain Nafion.

3.1. FT-IR of CsPWA

Fig. 2 reports the FT-IR measurement of prepared CsPWA. The primary Keggin structure is close to pure PWA [99]. Characteristics bands were observed at 1082, 985, 893 and 800 cm^{-1}. The bands at 1082, 893, and 800 cm^{-1} are assigned to starching vibration of P–O, W–O–W corner shared bond and W–O–W edges shared bond, respectively [100]. A split in W=O band at 985 cm^{-1} is seen which may be assigned to the interaction between $[PW_{12}O_{40}]^{3-}$ anion and Cs^+ cation [101].

3.2. SEM of powder

The SEM micrographs of prepared CsPWA powder are shown in Fig. 3. The powder was first grinded, dried at 80 °C and then subjected to the measurement. The very fine particles are clearly discerned (Fig. 3a). Agglomerate particles in the micrometric range are seen in Fig. 3b due to high hygroscopic property.

3.3. TGA, DTG and DSC

Fig. 4 compares the TGA–DTG responses of the prepared membranes. Three main weight losses [102], corresponding to major peaks in the DTG curves can be observed for each membrane. The onset and minimum temperatures related to these peaks are repre-

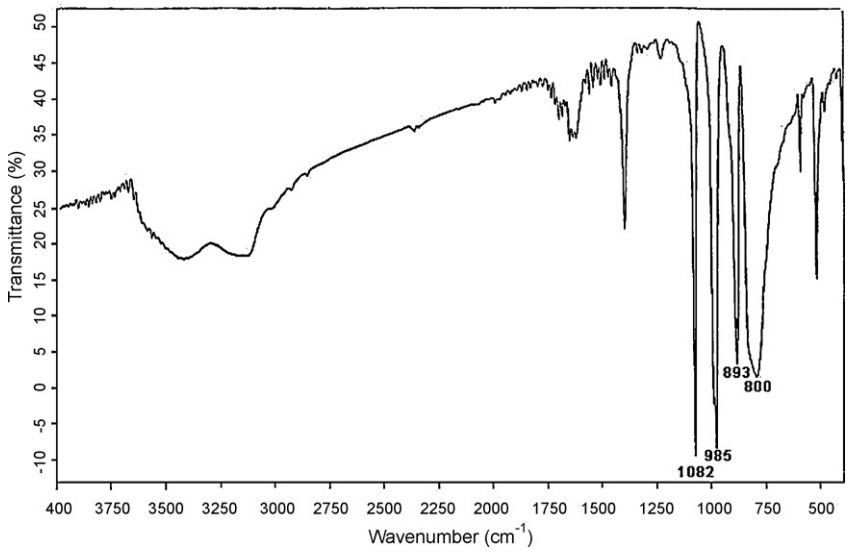

Fig. 2. FT-IR of the prepared CsPWA.

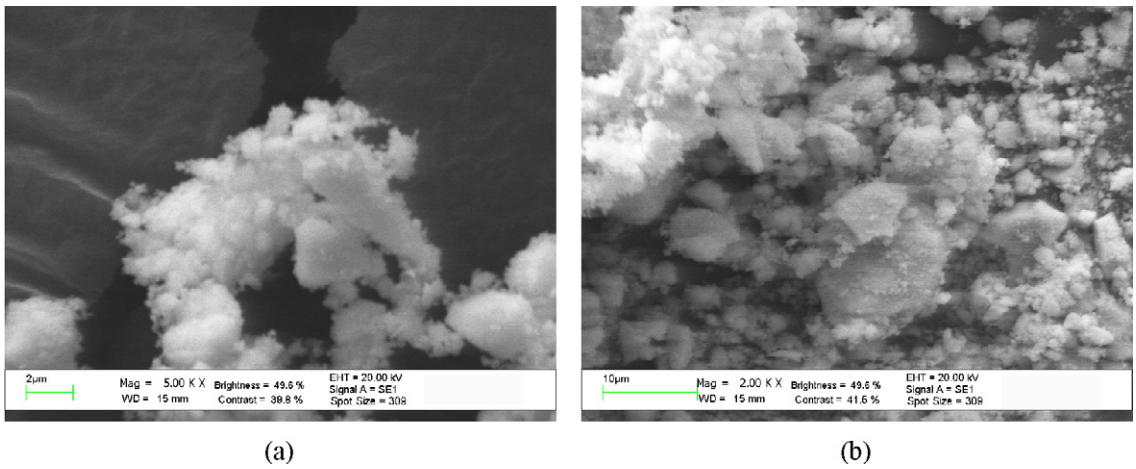

Fig. 3. SEM micrographs of the prepared CsPWA: (a) ×5000 and (b) ×2000.

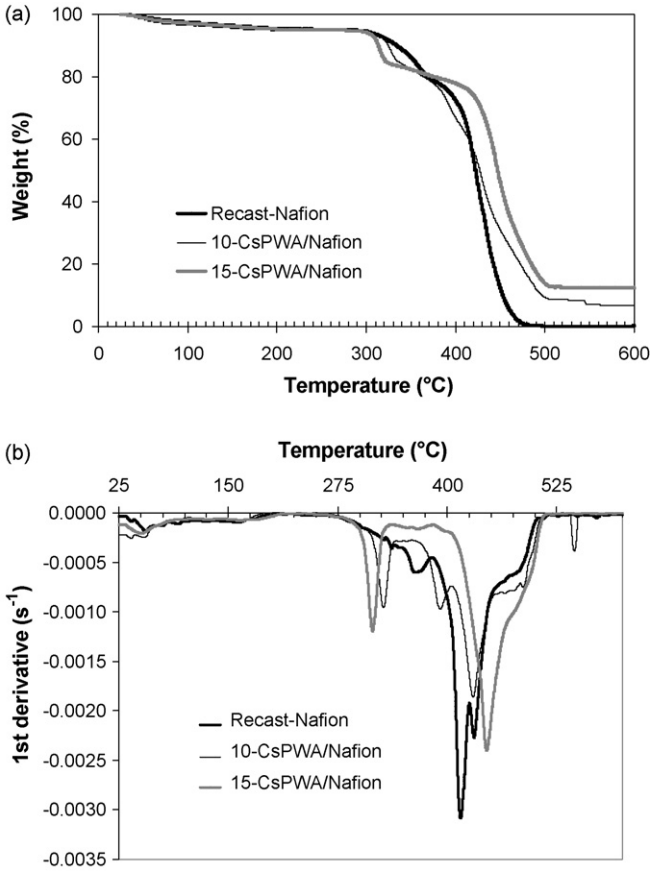

Fig. 4. Thermal gravimetric response of the prepared membranes: (a) TGA and (b) DTG.

sented in Table 3. Preliminary mass loss during the heating process from 25 to about 270 °C may be attributed to the evaporation of absorbed water molecules [56].

The first peak of the membranes weight loss was started at 270 °C. This peak is associated with the degradation of sulfonic acid groups [103]. The desulfonation rate of the nanocomposite membranes is faster than the Recast-Nafion membrane. In other word, CsPWA may catalytically increase the rate of desulfonation. The second weight loss may be attributed to decomposition of side-chain, while the third weight loss is related to decomposition of the PTFE backbone [29,104,105]. As seen in Table 3, the onset temperature of the second and third weight losses for the Recast-Nafion membrane is 380 °C and 426 °C. The onset temperatures for the second and third weight losses in the nanocomposite membranes are lower with faster mass losses than the bare Nafion; indicating the catalytic effect of CsPWA on the decomposition of Nafion. Although the decomposition mechanism of CF_2 backbone is not clear yet, the presence of CsPWA nanoparticles may accelerate the decomposition process. This effect is more vigorous when higher level (15%) of this salt was used. The decomposition of Nafion as the polymer matrix was finished at 520 °C. The residual mass above 600 °C in TGA curves is related to CsPWA.

Reduction of thermal stability for sulfonic acid groups and PTFE backbone of nanocomposites against plain Nafion membranes may indicate the interfacial interaction between CsPWA and Nafion. This interaction will be showed graphically in Section 3.5.

Fig. 5 shows the DSC traces of the prepared membranes. This figure reveals strong endothermic peaks around temperatures of 125–185 °C. These peaks may be associated with structural changes within the ionic clusters of membranes [104]. The onset and minimum transition temperature and enthalpy change, ΔH, corresponding to these peaks are reported in Table 3. These ΔH values may be related degree of hydration of Nafion-based membranes allowing high mobility of the chain segments [104]. In other

Table 3
Thermal properties (DTG, DSC) of the prepared membranes.

Entry	Membrane	DTG						DSC		
		Peak I		Peak II		Peak III		Peak		
		Desulfonation process		Side-chain decomposition		PTFE backbone decomposition		Structural changes		
		Onset (°C)	Min (°C)	Onset (°C)	Min (°C)	Onset (°C)	Min (°C)	Onset (°C)	Min (°C)	ΔH (J g_{Nafion}^{-1})
1	Recast-Nafion	270	368	380	416	426	431	124	153	202.8
2	10-CsPWA/Nafion	270	328	364	394	408	431	133	160	235.7
3	15-CsPWA/Nafion	270	316	338	362	387	446	133	152	102.7

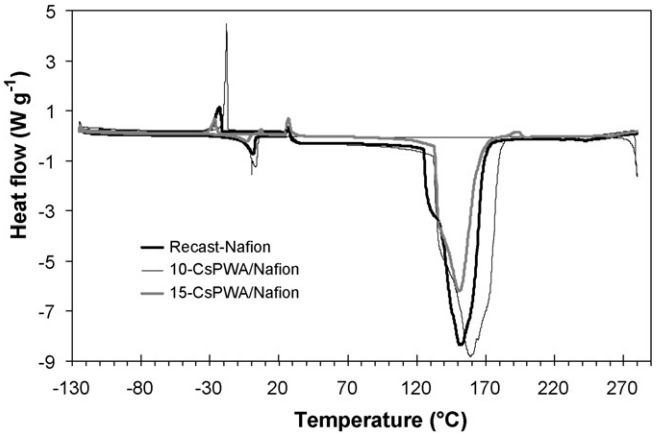

Fig. 5. Differential scanning calorimetry (DSC) of the prepared membranes.

word, ΔH values increase with increasing water content in the membrane. Sulfonic groups of the Nafion host polymer and the hygroscopic nature of CsPWA particles can serve to absorb more water through the nanocomposite membrane. Therefore, due to increase of water content in the membrane, the enthalpy change of 10-CsPWA/Nafion membrane is higher than plain Nafion. As demonstrated by Okuhara et al. [94], the particle size and crystallite size of CsPWA are 6.9 and 11.3 nm, respectively. The CsPWA particles size is not smaller than the Nafion cluster channels (~4 to 5 nm) [106] to entrap into them, so these particles are settled on the clusters. At higher level, CsPWA acts as a cover on the Nafion clusters resulting in decrease of the chain segments mobility or rather reduction in the free space in the membrane. Hence, the enthalpy change of 15-CsPWA/Nafion membrane is lower than others (see Table 3).

3.4. Water uptake and IEC

Water content in PEM fuel cells is important because it affects proton conductivity and overall system power [107]. The water uptake and IEC of prepared membranes are represented in Fig. 6. Interestingly, the water uptake of 10-CsPWA/Nafion membrane is higher than Recast-Nafion but decreased at higher level of CsPWA. The highest water uptake of nanocomposite membrane at 10% CsPWA may be associated with high hygroscopic nature of CsPWA. As a result, by increasing the level of CsPWA, the effect of covering Nafion sulfonic groups and agglomeration of salt particles may be the reason of reduction in water uptake. Similar trend has been reported by other authors [30,108]. Zhai et al. [30] applied sulfated-zirconia (S-ZrO_2) in Nafion matrix and observed a maximum water uptake in 10% S-ZrO_2.

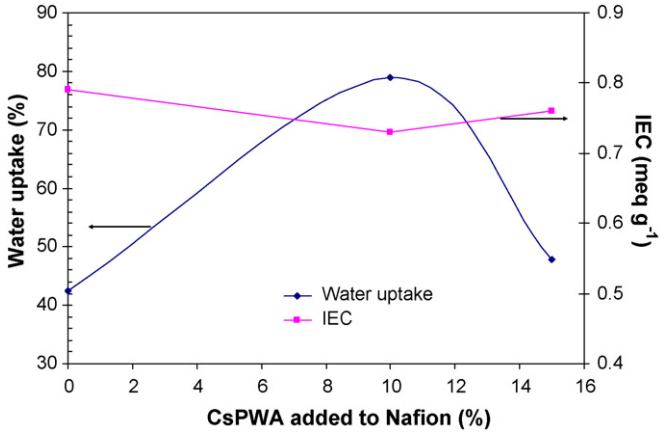

Fig. 6. Water uptake and IEC of the prepared membranes.

The IEC of nanocomposites is slightly lower than plain Nafion (Fig. 6.). This effect is due to covering [29] the Nafion active sites (sulfonic groups) and decreasing the effective number of replaceable ion exchange sites [73] by this salt. By adding the level of salt and in the presence of water, the proton generation reaction occurs and results in slight increase of the IEC. This reaction will be described in Section 3.5.

The IEC of Recast-Nafion membrane is smaller than commercial one (0.9 meq g^{-1}), and may be calculated on the basis of the equivalent weight of Nafion solution. The source of this discrepancy may be attributed to incomplete exchange of existing protons in the membrane with Na^+ ion [104] (refer Section 2).

3.5. Proton conductivity

For a solid electrolyte to be a good proton conductor, it should have fixed charged sites surrounded by water molecules, which facilitate the transport of protons [73]. The hydrophilicity, acid site density on inorganic nanoparticle surface, specific surface area of inorganic nanoparticles and amount of inorganic loading may have the influence on the conductivity of nanocomposite membrane [89].

Solid HPAs possess extremely high proton mobility [91]. Unlike the rigid network structure of zeolites, HPA Keggin anions are quite mobile [91]. Proton transport in Nafion nanocomposite membranes is the result of a complex process dominated by the surface and chemical properties of both Nafion and additive [8]. Due to high hydrophilicity of CsPWA, Nafion/CsPWA nanocomposite membrane is referred as hygroscopic and water substituted nanocomposite membrane [8].

Fig. 7 reveals the conductivity values against the relative humidity at 80 °C for the prepared membranes. The relative humidity is in the range of 30–100%. As seen in this figure, by increasing rela-

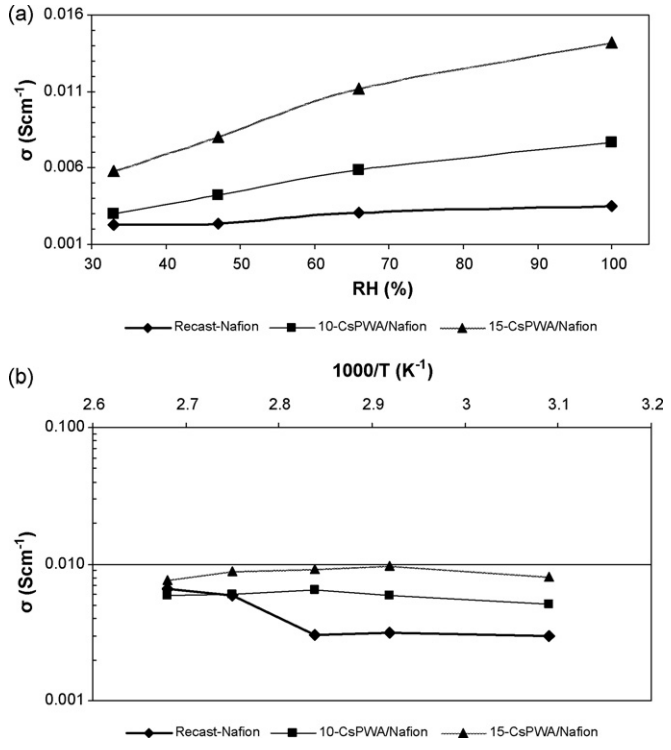

Fig. 7. Conductivity curves for the prepared membranes: (a) conductivity vs. relative humidity (RH) at 80 °C, (b) Arrhenius plot at 100% RH.

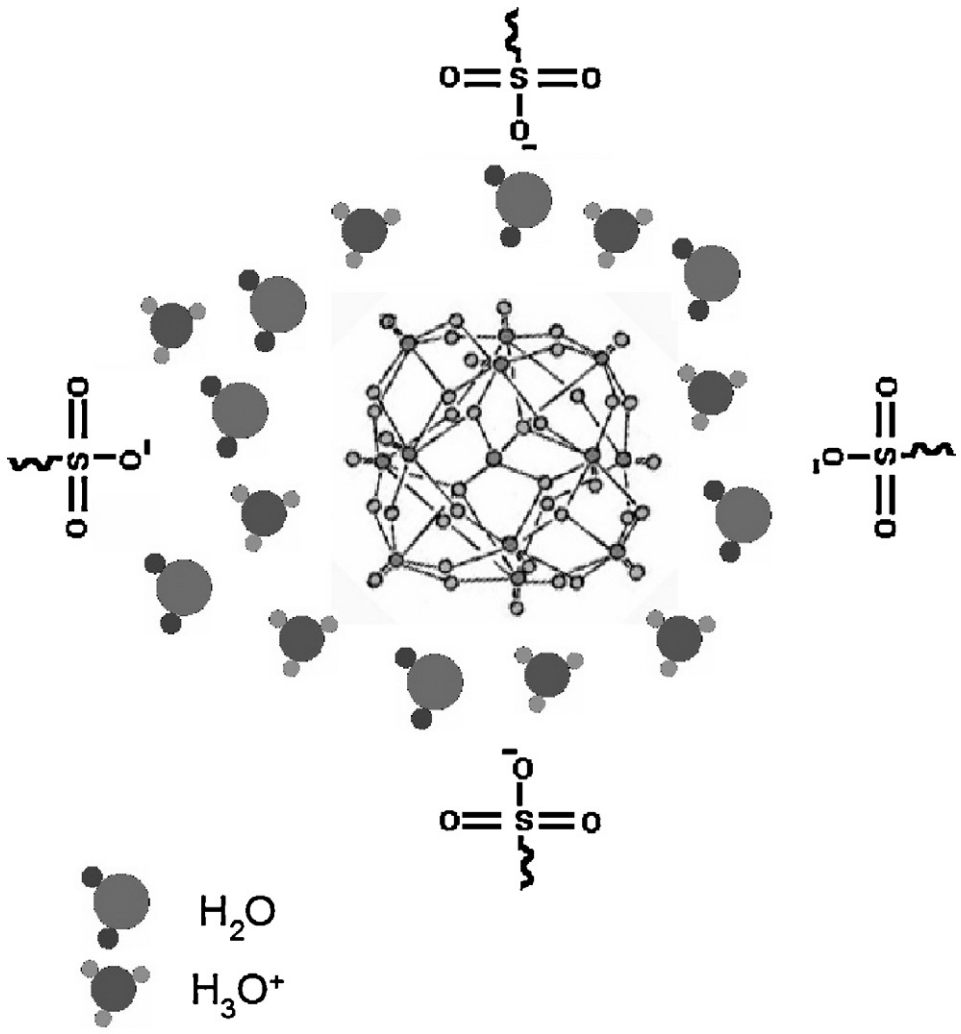

Fig. 8. Interactions between CsPWA with sulfonic groups of Nafion and water hydration molecules.

tive humidity, the conductivity is increasing but the conductivity of nanocomposite membranes is more sensitive to the humidity. The conductivity of 15-CsPWA/Nafion membrane increases one order of magnitude (from 5.80×10^{-3} to 1.42×10^{-2} S cm^{-1}) when the relative humidity changed from 30 to 100%.

The Arrhenius plot of the proton conductivity for the prepared membranes at 100% RH is presented in Fig. 7. The conductivity of membranes is in order of 10^{-3} and it may depend on the system, pretreatment, and equilibrium parameters used [8]. The conductivity of composite membranes is higher than Recast-Nafion membrane. The conductivity is increasing when the level of CsPWA is increased from 10 to 15%.

The ions transportation of Nafion membrane is governed by Grotthus and vehicle mechanisms [109]. CsPWA doped membrane promotes the molecular water absorption and favors the proton-conduction pathways [29]. The majority of absorbed water in 10-CsPWA/Nafion membrane may be surface water, which contributes less to proton conduction and act as resistance to vehicular mechanism [89]. The CsPWA can interact with the Nafion sulfonic groups and the water hydration molecules [110], forming a network of hydrogen bonds (see Fig. 8).

In the presence of water, the free proton may be formed by the reaction of anion moiety of CsPWA with the water molecule as described by Ukshe et al. [111]:

$$(PW_{12}O_{40})^{2.5-} + nH_2O \rightarrow [(PW_{12}O_{40})(OH)_x]^{(2.5+x)-} + xH^+ \quad (2)$$

The mechanism of proton conductivity in a given RH may be related to dynamic equilibrium between different proton moieties:

$$H_5O_2{}^+ \leftrightarrow H_3O^+ + H_2O \leftrightarrow H^+ + 2H_2O \quad (3)$$

Fig. 9 compares the conductivities of CsPWA added membranes with plain Nafion membrane at high temperatures (110 and 120 °C) and for 50% relative humidity. The figure indicates that the conduc-

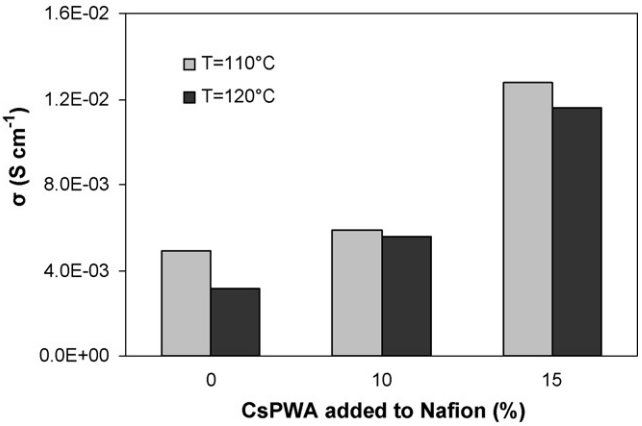

Fig. 9. Conductivities of membranes at high temperatures (110–120 °C) and 50% RH.

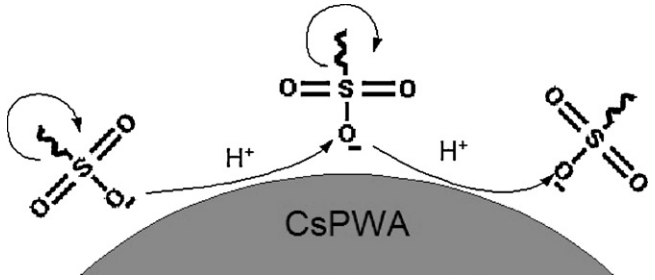

Fig. 10. The mechanism of proton transport at high temperature/low relative humidity at the interface of CsPWA and -SO_3H; Nafion backbone is not shown.

tivity of nanocomposite is higher than plain Nafion especially for the nanocomposite prepared by 15% CsPWA. The higher conductivity of composite membrane than plain Nafion membrane at higher temperatures may be related to additional water within the membrane and/or additional surface functional sites provided by CsPWA salt particles. The salt particles aid in holding water molecules tightly and impede the evaporation process during heating. The latter reason may be explained as follows.

Proton transport in the solid acid membranes can be either a bulk phenomena or a surface dominated process [8]. By virtue of the easy absorption, proton transport will occur on the surface of the crystalline HPA [91]. It may be considered that CsPWA nanoparticles provide additional surface functional sites for proton transfer in Nafion-composite membranes. The mechanism of this hypothesis can be illustrated in Fig. 10. The proton transport can occur from the $–SO_3H$ as proton donor to the $–SO_3^-$ as acceptor on the CsPWA surface. Since the $–SO_3H$ group has been fixed in the backbone, it constructs the closest packing structure on CsPWA surface [112].

3.6. PEM fuel cell test

The results of fuel cell tests of prepared membranes at different cell temperatures and humidity are summarized in Figs. 11–13. The thickness of Recast-Nafion and 10-CsPWA/Nafion membranes for fuel cell test are about 50–60 μm, so we can compare the performance of these two membranes and evaluate the effect of CsPWA additive on the fuel cell performance. Fig. 11 compares the fuel cell responses for those MEAs prepared by plain Nafion and 10% additive composite membranes at the cell temperatures of 50 and 70 °C. Two domains of humidity were considered including fully and partially humidification. The partially humidification was achieved by the difference between the cell and the inlet gases. In fully hydrated state and at high current densities, the cell with nanocomposite membrane has a better response than that cell with plain Nafion membrane. A bit higher overpotential in the region of 0–500 mA cm^{-2} is observed in the MEA prepared by 10-CsPWA/Nafion rather than Recast-Nafion at both temperatures of 50 and 70 °C under fully hydrated state (Fig. 11a and c). A maximum power density of 333 mW cm^{-2} at 720 mA cm^{-2} was achieved for the MEA prepared by 10-CsPWA/Nafion membrane at 70 °C and fully hydrated cell.

In partially hydrated cell, at low temperatures of 50 and 70 °C (Fig. 11b and d) and at high temperatures of 90 and 110 °C (Fig. 13a and b) the superior performance of the MEA prepared by nanocomposite membrane than plain Nafion is observed at both low and high current densities. This effect may be explained that at low rela-

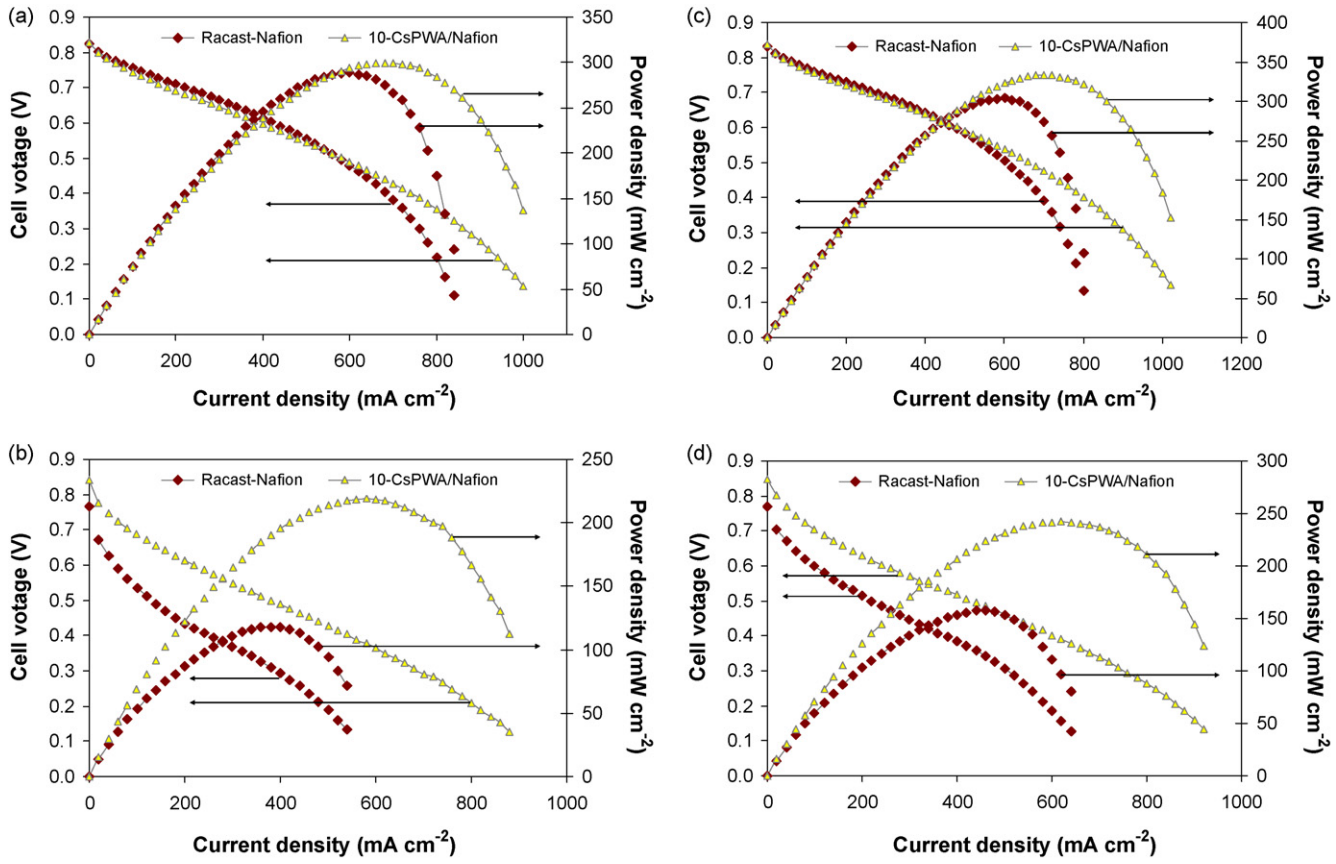

Fig. 11. Comparison of polarization and power–current curves between Recast-Nafion and 10-CsPWA/Nafion membranes at low cell temperature (T_{cell}) and inlet gas temperature (T_{gas}); (a) T_{cell} = 50 °C, T_{gas} = 50 °C (fully humidified), (b) T_{cell} = 50 °C, T_{gas} = 33 °C (partially humidified), (c) T_{cell} = 70 °C, T_{gas} = 70 °C (fully humidified), (d) T_{cell} = 70 °C, T_{gas} = 52 °C (partially humidified); membrane thickness 50–60 μm; anode and cathode gases H_2 and air at P = 1 atm.

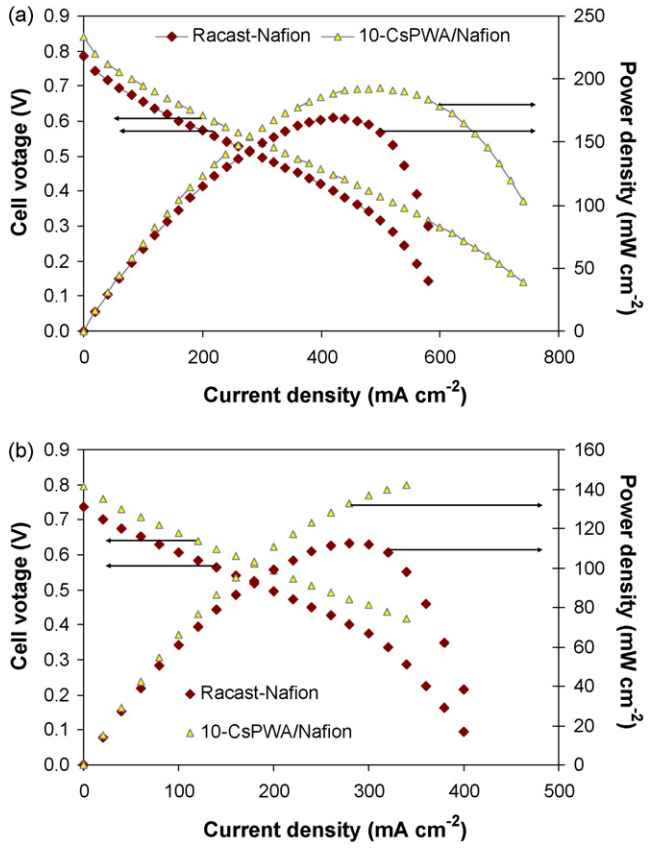

Fig. 12. Comparison of polarization and power–current curves between Recast-Nafion and 10-CsPWA/Nafion membranes at high cell temperature (T_{cell}) and inlet gas temperature (T_{gas}); (a) T_{cell} = 90 °C, T_{gas} = 73 °C (partially humidified), (b) T_{cell} = 110 °C, T_{gas} = 91 °C (partially humidified); membrane thickness 50–60 μm; anode and the cathode gases H_2 and air at P = 1 atm.

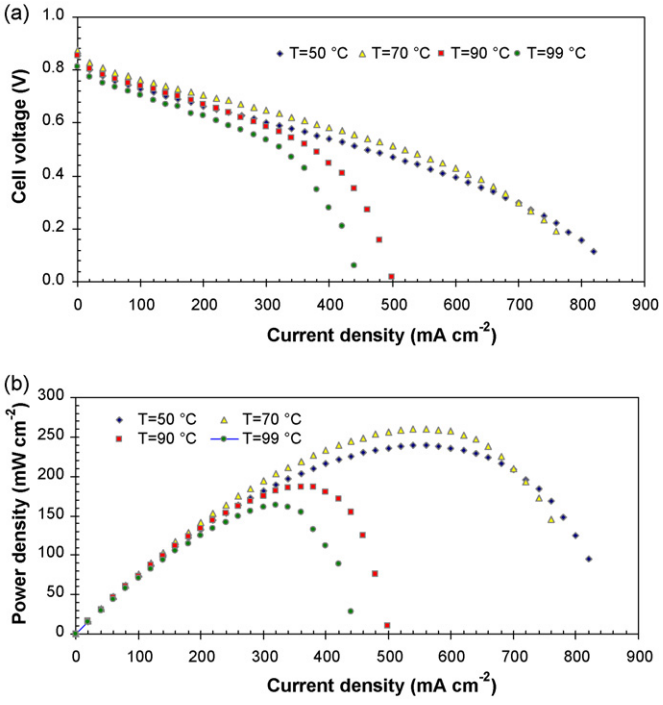

Fig. 13. Polarization (a) and power–current (b) curves of 15-CsPWA/Nafion membrane in fully humidified at different cell temperatures; membrane thickness 120 μm; anode and cathode gases H_2 and air at P = 1 atm.

tive humidity/high temperatures, the hydrophilic nature of CsPWA particles retained more water content and influences the water transfer to the cathode [113].

Fig. 13 reveals the polarization and power density of the MEA prepared by 15-CsPWA/Nafion membrane at different cell temperatures and fully saturated cell. Unexpectedly, the best response was obtained at the temperature of 70 °C and overall cell performance decreases with temperature increase from 70 to 99 °C. A maximum power density of 260 mW cm^{-2} at 560 mA cm^{-2} was achieved for this MEA.

4. Conclusion

In this study, CsPWA was used as a proton conducting additive to modify the Nafion membrane and produce stable nanocomposite at moderate temperature and low relative humidity. CsPWA/Nafion nanocomposite membranes were prepared by solution casting procedure.

The DSC traces of the prepared membranes revealed a strong endothermic peak around temperatures of 125–185 °C which may be associated with the structural changes within the ionic clusters of membranes. Enthalpy change, ΔH, corresponding to these peaks may be related to the degree of hydration of Nafion-based membranes allowing high mobility of the chain segments. The enthalpy change of 10-CsPWA/Nafion membrane is higher than plain Nafion due to increase of the water content in the nanocomposite membrane. Addition of more CsPWA particles (15%) may cover the clusters of Nafion resulting in decrease in the mobility of the chain segments or rather reduction of the free space in the membrane. This effect may reduce the enthalpy change.

The conductivity values at room temperature are in order of 10^{-3}. The conductivity of nanocomposite membranes at room temperature is slightly higher than plain Nafion. The conductivity of 15-CsPWA/Nafion membrane was increased one order of magnitude (from 5.80×10^{-3} to 1.42×10^{-2} S cm^{-1}) when the relative humidity was changed from 30 to 100%. The conductivity was improved when the level of CsPWA was increased from 10 to 15%. At high temperatures (110 and 120 °C), the conductivity of nanocomposite was higher compared to plain Nafion especially for the nanocomposite prepared by 15% CsPWA. The higher conductivity of nanocomposite membrane at higher temperatures may be attributed to the additional water within the nanocomposite membrane and/or the additional surface functional sites provided by CsPWA salt particles. The salt particles assist in tightly holding the water molecules and impede the evaporation process during heating. CsPWA nanoparticles may provide additional surface functional sites for proton transfer in Nafion-composite membranes. The proton transport can occur from the $-SO_3H$ as proton donor to the $-SO_3^-$ as acceptor on the CsPWA surface.

Comparison of the fuel cell responses of the MEAs prepared by Recast-Nafion and 10-CsPWA/Nafion membranes with the same thickness showed that in fully hydrated state and at higher current densities, the cell with nanocomposite membrane has a better response compared to plain Nafion. A bit higher overpotential in the region of 0–500 mA cm^{-2} was observed in the MEA prepared by 10-CsPWA/Nafion membrane rather than Recast-Nafion membrane at both temperatures of 50 and 70 °C under fully hydrated state. A maximum power density of 333 mW cm^{-2} at 720 mA cm^{-2} was achieved for the MEA prepared by 10-CsPWA/Nafion membrane at 70 °C and fully hydrated cell. In partially hydrated cell, at low temperatures of 50 and 70 °C and at high temperatures of 90 and 110 °C the superior performance of the MEA prepared by nanocomposite membrane compared to plain Nafion was observed at both low and high current densities. At low relative humidity/high temperatures, the hydrophilic nature of CsPWA particles retains more

water content and influences the water transfer to the cathode. The best response for the MEA prepared by 15-CsPWA/Nafion membrane at fully hydrated cell was obtained at the temperature of 70 °C. The overall cell performance was decreased with temperature increment from 70 to 99 °C. A maximum power density of 260 mW cm^{-2} at 560 mA cm^{-2} was achieved for this MEA.

Acknowledgement

The first author (M.A.) is grateful to Department of Chemistry, University of Rome "La Sapienza", Rome, Italy, for providing facilities to perform experiments.

References

[1] K.A. Mauritz, R.B. Moore, Chemical Review 104 (2004) 4535–4585.
[2] V. Neburchilov, J. Martin, H. Wang, J. Zhang, Journal of Power Sources 169 (2007) 221–238.
[3] J. Zhang, Z. Xie, J. Zhang, Y. Tang, C. Song, T. Navessin, Z. Shi, D. Song, H. Wang, D.P. Wilkinson, Z.-S. Liu, S. Holdcroft, Journal of Power Sources 160 (2006) 872–891.
[4] S. Licoccia, E. Traversa, Journal of Power Sources 159 (2006) 12–20.
[5] C. Yang, P. Costamagna, S. Srinivasan, J. Benziger, A.B. Bocarsly, Journal of Power Sources 103 (2001) 1–9.
[6] V. Ramani, H.R. Kunz, J.M. Fenton, Journal of Membrane Science 266 (2005) 110–114.
[7] O. Savadogo, Journal of Power Sources 127 (2004) 135–161.
[8] W.H.J. Hogarth, J.C. Diniz da Costa, G.Q.(Max) Lu, Journal of Power Sources 142 (2005) 223–237.
[9] K. Ramya, G. Velayutham, C.K. Subramaniam, N. Rajalakshmi, K.S. Dhathathreyan, Journal of Power Sources 160 (2006) 10–17.
[10] F. Liu, B. Yi, D. Xing, J. Yu, H. Zhang, Journal of Membrane Science 212 (2003) 213–223.
[11] T.L. Yu, H.-L. Lin, K.-S. Shen, L.-N. Huang, Y.-C. Chang, G.-B. Jung, J.C. Huang, Journal of Polymer Research 11 (2004) 217–224.
[12] J. Shim, H.Y. Ha, S.-A. Hong, I.-H. Oh, Journal of Power Sources 109 (2002) 412–417.
[13] H. Tang, X. Wang, M. Pan, F. Wang, Journal of Membrane Science 306 (2007) 298–306.
[14] P. Kongkachuichay, S. Pimprom, Chemical Engineering Research and Design 88 (2010) 496–500.
[15] H. Tian, O. Savadogo, Journal of New Materials for Electrochemical Systems 9 (2006) 61–71.
[16] V. Ramani, H.R. Kunz, J.M. Fenton, Journal of Membrane Science 232 (2004) 31–44.
[17] V. Ramani, H.R. Kunz, J.M. Fenton, Electrochimica Acta 50 (2005) 1181–1187.
[18] H. Tang, Z. Wan, M. Pan, S.P. Jiang, Electrochemistry Communications 9 (2007) 2003–2008.
[19] M.B. Satterfield, P.W. Majsztrik, H. Ota, J.B. Benziger, A.B. Bocarsly, Journal of Polymer Science: Part B: Polymer Physics 44 (2006) 2327–2345.
[20] E.I. Santiago, R.A. Isidoro, M.A. Dresch, B.R. Matos, M. Linardi, F.C. Fonseca, Electrochimica Acta 54 (2009) 4111–4117.
[21] B.R. Matos, E.M. Aricó, M. Linardi, A.S. Ferlauto, E.I. Santiago, F.C. Fonseca, Journal of Thermal Analysis and Calorimetry 97 (2009) 591–594.
[22] J. Pan, H. Zhang, W. Chen, M. Pan, International Journal of Hydrogen Energy 35 (2010) 2796–2801.
[23] N.H. Jalani, K. Dunn, R. Datta, Electrochimica Acta 51 (2005) 553–560.
[24] K.T. Adjemian, R. Dominey, L. Krishnan, H. Ota, P. Majsztrik, T. Zhang, J. Mann, B. Kirby, L. Gatto, M. Velo-Simpson, J. Leahy, S. Srinivasan, J.B. Benziger, A.B. Bocarsly, Chemistry of Materials 18 (2006) 2238–2248.
[25] Z.-G. Shao, H. Xu, M. Li, I.-M. Hsing, Solid State Ionics 177 (2006) 779–785.
[26] B.R. Matos, E.I. Santiago, F.C. Fonseca, M. Linardi, V. Lavayen, R.G. Lacerda, L.O. Ladeira, A.S. Ferlauto, Journal of The Electrochemical Society 154 (2007) B1358–B1361.
[27] F. Mura, R.F. Silva, A. Pozio, Electrochimica Acta 52 (2007) 5824–5828.
[28] H. Wang, B.A. Holmberg, L. Huang, Z. Wang, A. Mitra, J.M. Norbeck, Y. Yan, Journal of Materials Chemistry 12 (2002) 834–837.
[29] G.G. Kumar, A.R. Kim, K.S. Nahm, R. Elizabeth, International Journal of Hydrogen Energy 34 (2009) 9788–9794.
[30] Y. Zhai, H. Zhang, J. Hu, B. Yi, Journal of Membrane Science 280 (2006) 148–155.
[31] M.A. Navarra, C. Abbati, B. Scrosati, Journal of Power Sources 183 (2008) 109–113.
[32] Y. Kim, Y. Choi, H.K. Kim, J.S. Lee, Journal of Power Sources 195 (2010) 4653–4659.
[33] P. Bébin, M. Caravanier, H. Galiano, Journal of Membrane Science 278 (2006) 35–42.
[34] P. Costamagna, C. Yang, A.B. Bocarsly, S. Srinivasan, Electrochimica Acta 47 (2002) 1023–1033.
[35] C. Yang, S. Srinivasan, A.B. Bocarsly, S. Tulyani, J.B. Benziger, Journal of Membrane Science 237 (2004) 145–161.
[36] Y.-T. Kim, M.-K. Song, K.-H. Kim, S.-B. Park, S.-K. Min, H.-W. Rhee, Electrochimica Acta 50 (2004) 645–648.
[37] A.G. Kannan, N.R. Choudhury, N.K. Dutta, Journal of Membrane Science 333 (2009) 50–58.
[38] Y.S. Park, T. Hatae, H. Itoh, M.Y. Jang, Y. Yamazaki, Electrochimica Acta 50 (2004) 595–599.
[39] K. Tasaki, R. DeSousa, H. Wang, J. Gasa, A. Venkatesan, P. Pugazhendhi, R.O. Loutfy, Journal of Membrane Science 281 (2006) 570–580.
[40] Z.-G. Shao, P. Joghee, I.-M. Hsing, Journal of Membrane Science 229 (2004) 43–51.
[41] A. Mahreni, A.B. Mohamad, A.A.H. Kadhum, W.R.W. Daud, S.E. Iyuke, Journal of Membrane Science 327 (2009) 32–40.
[42] V. Ramani, H.R. Kunz, J.M. Fenton, Journal of Membrane Science 279 (2006) 506–512.
[43] X.-M. Yan, P. Mei, Y. Mi, L. Gao, S. Qin, Electrochemistry Communications 11 (2009) 71–74.
[44] S. Thayumanasundaram, M. Piga, S. Lavina, E. Negro, M. Jeyapandian, L. Ghassemzadeh, K. Müller, V. Di Noto, Electrochimica Acta 55 (2010) 1355–1365.
[45] H. Hagihara, H. Uchida, M. Watanabe, Electrochimica Acta 51 (2006) 3979–3985.
[46] H.W. Rollins, T. Whiteside, G.J. Shafer, J.-J. Ma, M.-H. Tu, J.-T. Liu, D.D. DesMarteau, Y.-P. Sun, Journal of Materials Chemistry 10 (2000) 2081–2084.
[47] C.-H. Wan, C.-L. Chen, International Journal of Hydrogen Energy 34 (2009) 9515–9522.
[48] Y. Liu, T. Nguyen, N. Kristian, Y. Yu, X. Wang, Journal of Membrane Science 330 (2009) 357–362.
[49] M. Aparicio, F. Damay, L.C. Klein, Journal of Sol–Gel Science and Technology 26 (2003) 1055–1059.
[50] J. Yang, P.K. Shen, J. Varcoe, Z. Wei, Journal of Power Sources 189 (2009) 1016–1019.
[51] S. Moravcová, Z. Cílová, K. Bouzek, Journal of Applied Electrochemistry 35 (2005) 991–997.
[52] R. Jiang, H.R. Kunz, J.M. Fenton, Journal of Membrane Science 272 (2006) 116–124.
[53] D.H. Jung, S.Y. Cho, D.H. Peck, D.R. Shin, J.S. Kim, Journal of Power Sources 106 (2002) 173–177.
[54] P.L. Antonucci, A.S. Aricò, P. Cretì, E. Ramunni, V. Antonucci, Solid State Ionics 125 (1999) 431–437.
[55] S. Ren, G. Sun, C. Li a, Z. Liang, Z. Wu, W. Jin, X. Qin, X. Yang, Journal of Membrane Science 282 (2006) 450–455.
[56] T. Li, Y. Yang, Journal of Power Sources 187 (2009) 332–340.
[57] F. Bauer, M. Willert-Porada, Journal of Membrane Science 233 (2004) 141–149.
[58] C. Arbizzani, A. Donnadio, M. Pica, M. Sganappa, A. Varzi, M. Casciola, M. Mastragostino, Journal of Power Sources 195 (2010) 7751–7756.
[59] Y.-S. Park, Y. Yamazaki, Solid State Ionics 176 (2005) 1079–1089.
[60] A.K. Sahu, S.D. Bhat, S. Pitchumani, P. Sridhar, V. Vimalan, C. George, N. Chandrakumar, A.K. Shukla, Journal of Membrane Science 345 (2009) 305–314.
[61] Y. Daiko, L.C. Klein, T. Kasuga, M. Nogami, Journal of Membrane Science 281 (2006) 619–625.
[62] C. Li, G. Sun, S. Ren, J. Liu, Q. Wang, Z. Wu, H. Sun, W. Jin, Journal of Membrane Science 272 (2006) 50–57.
[63] Z.X. Liang, T.S. Zhao, J. Prabhuram, Journal of Membrane Science 283 (2006) 219–224.
[64] C.H. Rhee, Y. Kim, J.S. Lee, H.K. Kim, H. Chang, Journal of Power Sources 159 (2006) 1015–1024.
[65] V. Saarinen, M. Karesoja, T. Kallio, M. Paronen, K. Kontturi, Journal of Membrane Science 280 (2006) 20–28.
[66] H.-L. Lin, T.L. Yu, L.-N. Huang, L.-C. Chen, K.-S. Shen, G.-B. Jung, Journal of Power Sources 150 (2005) 11–19.
[67] L.-N. Huang, L.-C. Chen, T.L. Yu, H. -Li Lin, Journal of Power Sources 161 (2006) 1096–1105.
[68] L.-C. Chen, T.L. Yu, H.-L. Lin, S.-H. Yeh, Journal of Membrane Science 307 (2008) 10–20.
[69] M.H. Yildirim, A.R. Curoś, J. Motuzas, A. Julbe, D.F. Stamatialis, M. Wessling, Journal of Membrane Science 338 (2009) 75–83.
[70] R.H. Alonso, L. Estevez, H. Lian, A. Kelarakis, E.P. Giannelis, Polymer 50 (2009) 2402–2410.
[71] D.H. Jung, S.Y. Choa, D.H. Peck, D.R. Shin, J.S. Kim, Journal of Power Sources 118 (2003) 205–211.
[72] M.M. Hasani-Sadrabadi, E. Dashtimoghadam, F.S. Majedi, K. Kabiri, Journal of Power Sources 190 (2009) 318–321.
[73] L. Barbora, S. Acharya, R. Singh, K. Scott, A. Verma, Journal of Membrane Science 326 (2009) 721–726.
[74] M.A. Smit, A.L. Ocampo, M.A. Espinosa-Medina, P.J. Sebastián, Journal of Power Sources 124 (2003) 59–64.
[75] J. Zhu, R.R. Sattler, A. Garsuch, O. Yepez, P.G. Pickup, Electrochimica Acta 51 (2006) 4052–4060.
[76] H.S. Park, Y.J. Kim, W.H. Hong, H.K. Lee, Journal of Membrane Science 272 (2006) 28–36.
[77] D. Liu, M.Z. Yates, Journal of Membrane Science 326 (2009) 539–548.
[78] C.-H. Wang, C.-C. Chen, H.-C. Hsu, H.-Y. Du, C.-P. Chen, J.-Y. Hwang, L.C. Chen, H.-C. Shih, J. Stejskal, K.H. Chen, Journal of Power Sources 190 (2009) 279–284.

[79] R. Wycisk, J. Chisholm, J. Lee, J. Lin, P.N. Pintauro, Journal of Power Sources 163 (2006) 9–17.
[80] J. Liu, H. Wang, S. Cheng, K.-Y. Chan, Journal of Membrane Science 246 (2005) 95–101.
[81] T. Nguyen, X. Wang, Journal of Power Sources 195 (2010) 1024–1030.
[82] B.P. Ladewig, R.B. Knott, D.J. Martin, J.C. Diniz da Costa, G.Q. Lu, Electrochemistry Communications 9 (2007) 781–786.
[83] H. Lin, C. Zhao, H. Na, Journal of Power Sources 195 (2010) 3380–3385.
[84] H. Kim, M.-S. Kang, D.H. Lee, J. Won, J. Kim, Y.S. Kang, Journal of Membrane Science 304 (2007) 60–64.
[85] C.-Y. Chen, J.I. Garnica-Rodriguez, M.C. Duke, R.F. Dalla Costa, A.L. Dicks, J.C. Diniz da Costa, Journal of Power Sources 166 (2007) 324–330.
[86] Y. Zhang, Z. Cui, C. Liu, W. Xing, J. Zhang, Journal of Power Sources 194 (2009) 730–736.
[87] Y. Fang, T. Wang, R. Miao, L. Tang, X. Wang, Electrochimica Acta 55 (2010) 2404–2408.
[88] G. Alberti, M. Casciola, Annual Review of Materials Science 33 (2003) 129–154.
[89] P. Choi, N.H. Jalani, T.M. Thampan, R. Datta, Journal of Polymer Science: Part B: Polymer Physics 44 (2006) 2183–2200.
[90] U.B. Mioč, M.R. Todorović, M. Davidović, Ph. Colomban, I. Holclajtner-Antunović, Solid State Ionics 176 (2005) 3005–3017.
[91] I.V. Kozhevnikov, Chemical Reviews 98 (1998) 171–198.
[92] N. Mizuno, M. Misono, Chemical Reviews 98 (1998) 199–217.
[93] T. Okuhara, Catalysis Today 73 (2002) 167–176.
[94] T. Okuhara, H. Watanabe, T. Nishimura, K. Inumaru, M. Misono, Chemistry of Materials 12 (2000) 2230–2238.
[95] K.Y. Lee, N. Mizuno, T. Okuhara, M. Misono, Bulletin of the Chemical Society of Japan 62 (1989) 1731–1739.
[96] E.F. Kozhevnikova, E. Rafiee, I.V. Kozhevnikov, Applied Catalysis A: General 260 (2004) 25–34.
[97] E. Rafiee, Z. Zolfagharifar, M. Joshaghani, S. Eavani, Applied Catalysis A: General 365 (2009) 287–291.
[98] K. Na, T. Iizaki, T. Okuhara, M. Misono, Journal of Molecular Catalysis A: Chemical 115 (1997) 449–455.
[99] L. Wang, B.L. Yi, H.M. Zhang, D.M. Xing, Electrochimica Acta 52 (2007) 5479–5483.
[100] C. Rocchiccioli-Deltcheff, M. Fournier, R. Franck, R. Thouvenot, Inorganic Chemistry 22 (1983) 207–216.
[101] L.R. Pizzio, M.N. Blanco, Applied Catalysis A: General 255 (2003) 265–277.
[102] S.H. de Almeida, Y. Kawano, Journal of Thermal Analysis and Calorimetry 58 (1999) 569–577.
[103] J.Y. Xi, Z.H. Wu, X.P. Qiu, L.Q. Chen, Journal of Power Sources 166 (2007) 531–536.
[104] M.A. Navarra, F. Croce, B. Scrosati, Journal of Materials Chemistry 17 (2007) 3210–3215.
[105] V. Di Noto, S. Lavina, E. Negro, M. Vittadello, F. Conti, M. Piga, G. Pace, Journal of Power Sources 187 (2009) 57–66.
[106] W.Y. Hsu, T.D. Gierke, Journal of Membrane Science 13 (1983) 307–326.
[107] M.A. Hickner, H. Ghassemi, Y.S. Kim, B.R. Einsla, J.E. McGrath, Chemical Reviews 104 (2004) 4587–4612.
[108] M.H.D. Othman, A.F. Ismail, A. Mustafa, Journal of Membrane Science 299 (2007) 156–165.
[109] K.D. Kreuer, Journal of Membrane Science 185 (2001) 29–39.
[110] E. Fontananova, F. Trotta, J.C. Jansen, E. Drioli, Journal of Membrane Science 348 (2010) 326–336.
[111] E.A. Ukshe, L.S. Leonova, A.I. Korosteleva, Solid State Ionics 36 (1989) 219–223.
[112] M. Yamada, I. Honma, Journal of Physical Chemistry B 110 (2006) 20486–20490.
[113] S. Vengatesan, H.-J. Kim, S.-Y. Lee, E.A. Cho, H.Y. Ha, I.-H. Oh, T.-H. Lim, Journal of Power Sources 167 (2007) 325–329.